Spontaneous Fission Fragment Velocity Measurements and Coincident Gamma Spectra for Cf^{252}

J. C. D. MILTON AND J. S. FRASER
Chalk River Laboratories, Atomic Energy of Canada Limited, Chalk River, Ontario, Canada
(Received February 3, 1958)

The velocities of both fission fragments from the spontaneous fission of Cf^{252} have been measured simultaneously with the pulse-height spectrum produced by the fission gamma rays in a large NaI(Tl) crystal. The average total kinetic energy before neutron emission is found to be 181.9 Mev with a full width at half-maximum of 17.5 Mev at the most probable mass ratio 1.33. The width has been corrected for neutron recoil and the average total kinetic energy for the effect of the angular dispersion of the fragments by neutrons. The yield of gamma rays shows a pronounced dip in the region where one of the fragments is near the doubly magic nucleus Sn^{132}. There is a suggestion that the average gamma-ray energy is higher in this region. The correlation in number of gamma rays with total kinetic energy is very small and can be represented by

$$\frac{1}{\langle N_\gamma \rangle}\frac{dN_\gamma}{dE_T}=-0.0029_{-0.0011}{}^{+0.0007}\ \text{Mev}^{-1}.$$

INTRODUCTION

THE earliest detailed accurate studies of fission kinetics were made by Brunton and Hanna[1] and Brunton and Thompson,[2] using double back-to-back ionization chambers and multiple-channel pulse-height analyzers. Because of the uncertainties in energy calibration and energy dispersion, many experimenters have been led to use time-of-flight techniques,[3–5] which have fundamentally much greater accuracy but much lower efficiency because of the small solid angles which must be used. In principle the fragment velocity may be measured more and more accurately by increasing the flight path, but, in fact, the precision of the velocity measurements is limited to about three percent by the spread introduced by the recoil of the departing neutrons unless the neutron angle and energy are simultaneously measured.

APPARATUS

A full description of the apparatus is being published separately.[6] Briefly, the apparatus (see Fig. 1) records on punched tape the flight times of both fission fragments over two similar 182.5-cm flight paths and the pulse height produced by gamma rays coincident with the fission event in a 4-in. diameter by 4-in. thick NaI(Tl) crystal mounted at 90° to the drift tube axis and with its front face 10 cm from the source. The apparatus functions as a three-dimensional analyzer of up to 100-channel capacity in each dimension. After transferring the information to punched cards, all subsequent data-processing was done on the Chalk River Datatron. The size of the memory in this computer (4000 words) forced us to restrict the range of the analyzer to 60 channels in each dimension so that sorts could be made by taking two variables at a time.

The zero-time signal was obtained by collecting and accelerating the electrons ejected by one of the fragments from a thin foil mounted close to the source. This technique was first suggested by Stein and Leachman.[7] In this experiment the foil consisted of 8 $\mu g/cm^2$ VYNS[8] onto which had been evaporated 8 $\mu g/cm^2$ of gold. The foil was mounted at 45° to the drift tube axis so that a fragment lost about 1 Mev in traversing it.

The foil used as the source backing was made identical to the start foil; it was mounted at 90° to the beam axis. A weightless source of Cf^{252} giving 3×10^4 fissions per minute was deposited on the backing by room temperature sublimation. This procedure is made possible by the intense local heating produced by a fission fragment. A few thousand californium atoms may be evaporated for every fragment whose path intersects the surface.[9] We are very much indebted to Dr. S. G. Thompson and Dr. T. Sikkeland of the University of California Radiation Laboratory for preparing this excellent source and allowing us to make use of their Cf^{252}.

The fragments were detected at the end of the flight path by two identical 4-in. diameter thin plastic phosphors. Each subtended a solid angle of 1.94×10^{-4} of 4π at the source.

A pulse in the gamma detector was not required to initiate recording, but when a triple coincidence occurred between the start and two stop pulses a gate was opened in the gamma channel. This channel was set to record the pulse-height range 0.2 to 1.4 Mev in

[1] D. C. Brunton and G. C. Hanna, Can. J. Research **A28**, 190 (1950).
[2] D. C. Brunton and W. B. Thompson, Can. J. Research, **28A**, 498 (1950).
[3] H. W. Schmitt and R. B. Leachman, Phys. Rev. **102**, 183 (1956).
[4] W. E. Stein, Phys. Rev. **108**, 94 (1957), and private communication.
[5] W. E. Stein and S. L. Whetstone, Phys. Rev. **110**, 476 (1958).
[6] J. S. Fraser and J. C. D. Milton, Nuclear Instr. **2**, 275 (1958).
[7] W. E. Stein and R. B. Leachman, Rev. Sci. Instr. **27**, 1049 (1956).
[8] A vinyl chloride-acetate polymer obtainable from Canadian Resins and Chemicals Limited, Montreal, Canada.
[9] B. V. Ershler and F. S. Lapteva, Atomnaya Energiya **1**, No. 4, 63 (1956) [translation: J. Nuclear Energy **4**, 471 (1957)].

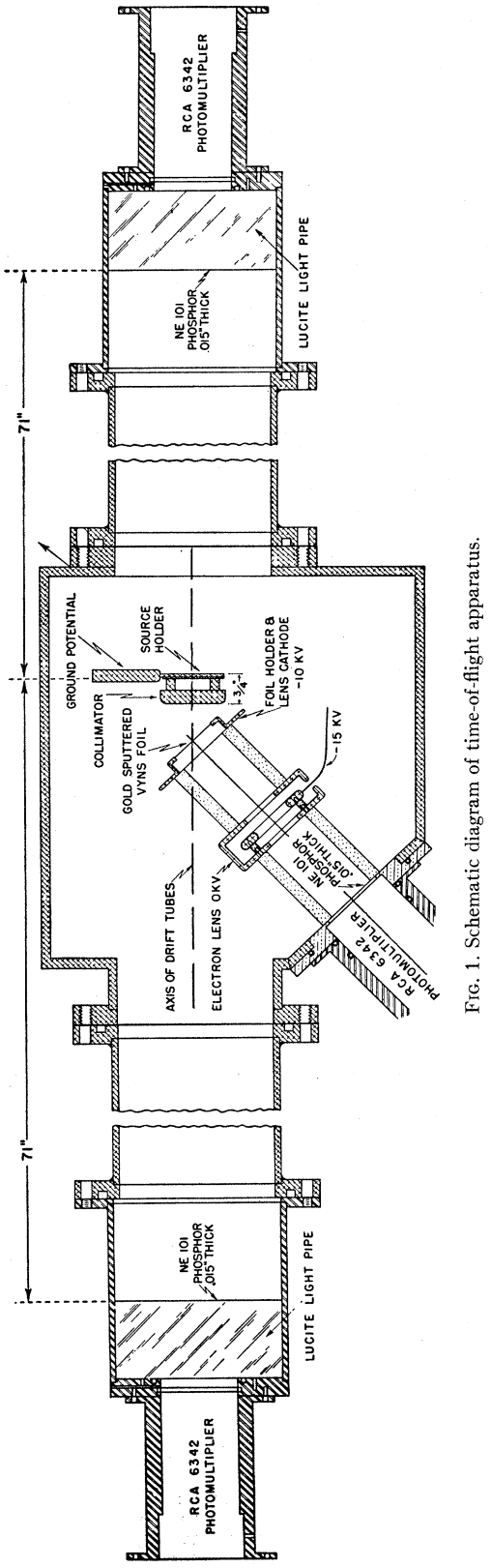

FIG. 1. Schematic diagram of time-of-flight apparatus.

59 channels with all pulse heights larger than 1.4 Mev going into a 60th channel. The fragment timing channels covered the range 107 to 236×10^{-9} sec with a channel width of 2.1×10^{-9} sec.

CALIBRATION AND CORRECTIONS

The zero of the time scale was found by measuring the position in time of the light- and heavy-fragment peaks as a function of the distance from the source to the appropriate detector and extrapolating to zero distance. A detailed description of the calibration procedure is given elsewhere.[6] For the purpose of this paper it is sufficient to say that the source was oriented in the apparatus so that one of the fragments passed through both foils, the other passed through neither. The correction for source and start foil losses was then made by adjusting the time scale for the group of fragments which had traversed the foils so that the most probable light- and heavy-fragment velocities

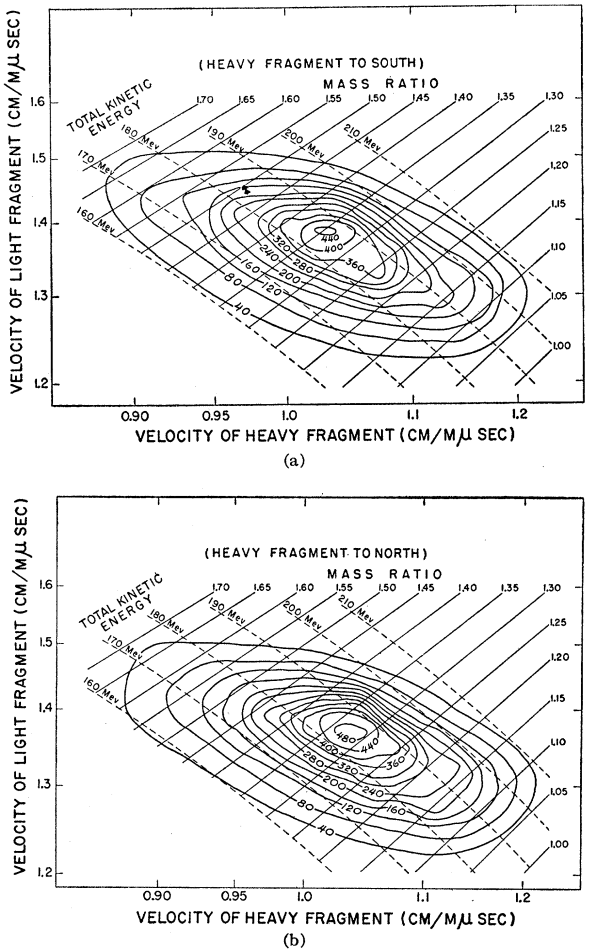

FIG. 2(a). Time-interval contour plot for heavy fragment to the south. The number on each contour represents the actual number of events in a box 2.1 mμsec on edge. (b) Time-interval contour plot for heavy fragment to the north.

were the same as those for the group which had not traversed either foil. The correction amounted to 2.5 Mev per fragment. The calculated loss from the known foil thicknesses was 1.8±0.3 Mev.

This procedure assumes that the source itself has no thickness, which is certainly true, and that the californium atoms have not penetrated appreciably into the backing, which is probably correct.

FRAGMENT VELOCITY MEASUREMENTS

About 85 500 events were recorded at 5.5 counts per minute. Of these, 21 300 had gamma pulses greater than 200 kev.

The fragment-fragment correlation data are shown in Figs. 2(a) and 2(b), representing the results from the two sides of the apparatus (referred to as north and south). Because of the slightly differing calibrations of the two sides it is not convenient at this stage to combine the data. The figures are time-interval contour plots similar to those commonly employed,[1,2] except that the altitude represents the probability of obtaining an event in the interval $\Delta t_L \Delta t_H$ rather than $\Delta E_L \Delta E_H$ as in the ionization chamber work. On the time-interval plot as compared to the energy-interval one, the peak is shifted one to two Mev higher in total kinetic energy E_T and the high-E_T side of the mountain is steeper.

The small irregularities in the contours are not significant. They result from the first-order difference method used by the computer in finding the contour intersections. However, the bump at the low-mass-ratio end of the ridge is thought to be significant and is probably due to the influence of the doubly magic 50 proton—82 neutron core on the probability of formation of the primary fission fragments. A mass splitting of 132–120 would occur at mass ratio 1.10.

This feature may be seen, perhaps more clearly, in the prompt mass yields (Fig. 3). The mass resolution in this experiment is shown in Table I. The spread in mass due to neutron emission, ΔM_n, is derived in Appendix A. The spread due to time resolution, ΔM_t, is calculated for the most probable mode at the indicated mass ratio using $\Delta t = 3.5$ mμsec, and is assumed to add in quadrature with the neutron recoil spread. Since the neutron spread is so large there is no point in increasing the fragment flight path beyond 182 cm, unless the directions and energies of the neutrons are simultaneously measured. Doubling the flight path results in only a 22% improvement in mass resolution while cutting the counting rate to $\frac{1}{4}$.

As observed in the yields of the lower mass number fissionable nuclides U^{233}, U^{235}, and Pu^{239}, the position of the heavy-fragment peak remains constant while the change in mass is taken care of by a shift of the light peak. In Cf^{252} there is a tendency for the heavy peak to move slightly toward higher masses.

Although the statistical accuracy of the chemical data[10] is poor the agreement is quite good. As would be expected with a mass resolution of three units our peaks appear to be somewhat broader.

TABLE I. Mass resolution, ΔM, full width at half-maximum in mass units. ΔM_n is the contribution of neutron recoil and ΔM_t the contribution of time spread (see text).

$R = M_H/M_L$	ΔM_n	ΔM_t	ΔM
1.0	1.98	2.10	2.89
1.3	1.94	2.05	2.82
1.5	1.90	1.98	2.74

In Fig. 4, we show several features as functions of the mass ratio. The most probable prompt mass ratio is 1.33. The prompt total kinetic energy averaged over all modes is 181.9±5.0 Mev, after making a correction of −0.8±0.4 Mev for the change in detection efficiency with the number of neutrons emitted (see Appendix B). In finding the average total kinetic energy, 1100 events with energies less than 140 or greater than 225 Mev were rejected. These spurious background events amounted to about $\frac{1}{2}$ count per cell. To find proper averages in the presence of such a small background it is not necessary to subtract out the background, but only to do the averaging between limits which are symmetrically placed about the distribution, provided the distribution is itself sufficiently symmetric.

We may calculate the average total excitation energy if we know the total energy released, i.e., if we know the masses of the prompt fragments. Using the mass formula of Cameron,[11] we have calculated the values of the maximum energy release shown by the set of points in Fig. 4(c). The average energy available will be somewhat smaller and may even be considerably smaller if the most probable charge splitting differs

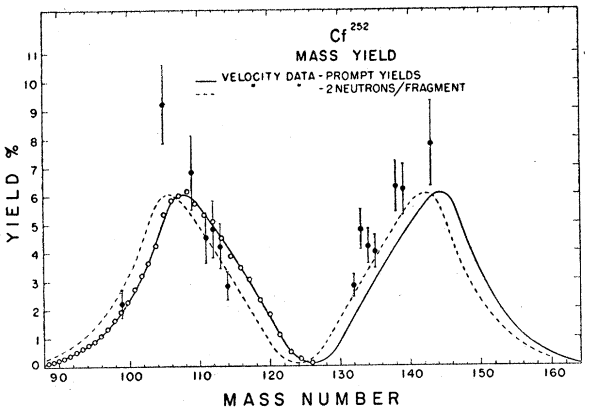

FIG. 3. Prompt mass yields (open circles and solid curve) compared with the radiochemical data (solid circles) of Glendenin and Steinberg.[10] The dotted line is the resultant yield curve assuming two neutrons emitted from each fragment.

[10] L. E. Glendenin and E. P. Steinberg, J. Inorg. Nuclear Chem. 1, 45 (1955).

[11] A. G. W. Cameron, Chalk River Laboratory Report CRP-690 (unpublished) and Can. J. Phys. 35, 1021 (1957).

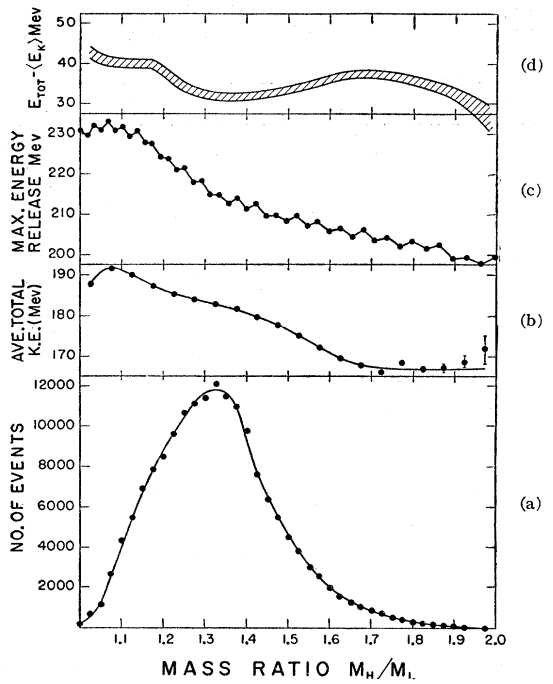

FIG. 4(a). Mass-ratio distribution for Cf^{252}. In this and many of the succeeding curves the experimental data appear doubled. In this case all events were sorted into mass-ratio intervals $\Delta R=0.05$ spaced 0.025 apart. This procedure improves the smoothing. (b) Average total kinetic energy, $\langle E_K\rangle$, as a function of mass ratio. (c) Maximum prompt energy release using the masses given by the formula of Cameron.[11] (d) Upper limit for the average total excitation energy of both fragments.

appreciably from the one which would give the maximum energy release. The difference between Figs. 4(c) and 4(b), plotted in Fig. 4(d), should then be regarded as an upper limit to the average excitation energy of both the fragments. The odd-even variations in energy release are contained within the shaded band. If the most probable charge division coincides with the maximum energy release, or nearly coincides as in the equal chain length hypothesis, then Fig. 4(d) represents the actual total excitation energy. If, in addition, the spread in charge is two units as in the fission of U^{235},[12] then the spread in energy release due to fluctuations in charge splitting is small, roughly two Mev.[13] If, however, the most probable charge division is shifted appreciably from the maximum to a steep region of the energy release curve, the width may be considerably greater; e.g., if the shift is 1.5 charge units, the width would be approximately 10 Mev instead of 2 Mev.

Assuming that the most probable charge division occurs at the maximum energy release, so that the spread in charge has a small contribution to the spread in total kinetic energies, it is a simple matter to derive distributions in total excitation energies, for each mass ratio, from the kinetic energy distributions given in Fig. 5, by making use of Fig. 4(c). The width of the total excitation energy distributions is found to be greatest at $R=1.10$ and 1.55 and least at 1.30. These widths must be corrected for the neutron recoil and time resolution which together contribute a spread $\Delta E/E=5.76\%$ (see Appendix A) at the most probable mass ratio. This spread varies slightly with mass ratio because of the dependence of $\langle\nu\rangle$ on E. In calculating the correction, a value of $\langle\nu\rangle$ appropriate to the average total kinetic energy at the mass ratio was used. Such a procedure is not quite correct because the resolution function varies considerably over each of the curves. Although this variation partially accounts for the asymmetry of the curves, its effect on the width correction is small. In Table II we list the full widths at half-maximum as measured from Fig. 5 with the corrected widths. The observed widths are thought to be good to ± 1 Mev.

TABLE II. Widths of total kinetic energy distribution.

R	ΔE (Mev)	W obs (Mev)	W corr. (Mev)
1.10	9.75	23.7	21.6
1.15	9.86	24.0	21.9
1.20	9.96	24.0	21.8
1.25	10.05	21.7	19.2
1.30	10.10	19.7	16.9
1.35	10.14	20.3	17.6
1.40	10.20	22.2	19.7
1.45	10.26	21.7	19.1
1.50	10.30	23.0	20.6
1.55	10.35	23.0	20.5

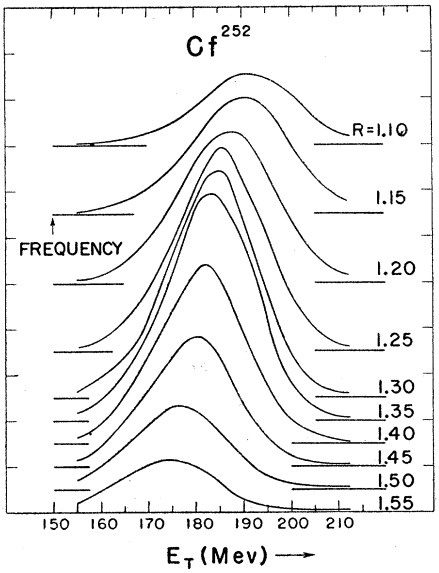

FIG. 5. Total kinetic-energy distribution as a function of mass ratio.

[12] A. E. Pappas, *Proceedings of the International Conference on the Peaceful Uses of Atomic Energy, Geneva, 1955* (United Nations, New York, 1956), Vol. 7, p. 19.

[13] Proceedings of Fission Symposium at Chalk River, Chalk River Laboratory Report CRP-642-A (unpublished), p. 209.

GAMMA-RAY MEASUREMENTS

The over-all gamma pulse-height spectrum is shown in Fig. 6. The spectrum was arbitrarily cut off at 200 kev (channel 5). Gamma-ray spectra were obtained for 18 mass-ratio intervals between 1.0 and 1.9, but no significant difference or trend could be discerned by eye. We have therefore made use of statistical considerations. A chi-squared test[14] was applied by comparing the 18 sample spectra with a population given by the observed average spectrum. The values of χ^2 for each individual sample lie close to the expected values (Fig. 7) but the over-all value of χ^2 for all 18 samples[14] is found to be very large. In fact the probability of finding a larger χ^2 than the observed one is 0.01%. On the other hand, a similar χ^2 test performed for the gamma spectra associated with 20 intervals in E_T gave a χ^2 almost equal to the expected value, i.e., the probability of getting a χ^2 larger than the observed one was 50%. We conclude then that the gamma spectrum does not vary significantly with E_T but does vary with R.

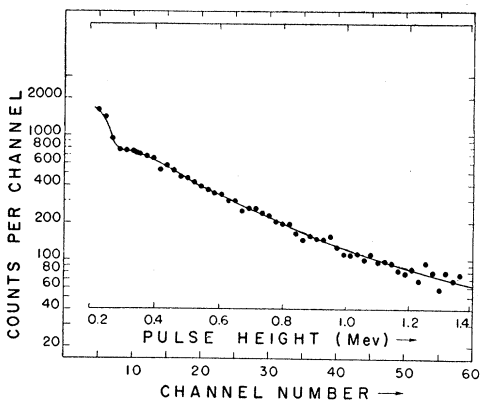

FIG. 6. Cf^{252} fission gamma-ray pulse-height spectrum in a 4-in. diameter by 4-in. thick NaI(Tl) crystal.

We next consider the gamma yield as a function of mass ratio. The yield is here defined as the number of gamma rays producing pulse heights in the crystal greater than 200 kev. In Fig. 8(b) a very pronounced decrease in the yield is observed at $R=1.1$. This is just the region where the heavy fragments have a small number of nucleons outside of the doubly magic core of 50 protons and 82 neutrons. Muehlhause[15] has observed that the neutron-capture gamma-ray multiplicity is low for a closed-shell nucleus.

The larger level spacings in fragments near closed shells should result in higher gamma-ray energies. The average height of all pulses lying between 200 and 1400 kev [Fig. 8(c)] suggests that the gamma rays are slightly more energetic near $R=1.1$.

The 50-neutron shell nuclei would be reached by a mass splitting of 1.86. Again there is a suggestion that the gamma yield is low and the average pulse height high, although there are very few events in this region.

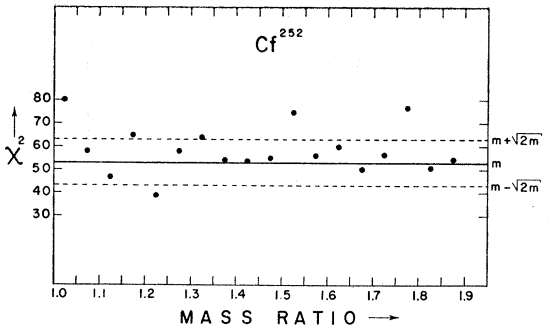

FIG. 7. Chi-squared test applied to gamma pulse-height spectra.

A similar treatment in terms of the total kinetic energy, E_T, showed that the yield of gamma rays decreased as E_T increased (Fig. 9). The decrease is, however, not nearly so striking as the decrease in the number of neutrons with increasing E_T found by Hicks *et al.*[5,16] The uncorrected experimental value is

$$\frac{1}{\langle N_\gamma \rangle}\frac{dN_\gamma}{dE_T}=-0.0033\ \text{Mev}^{-1}.$$

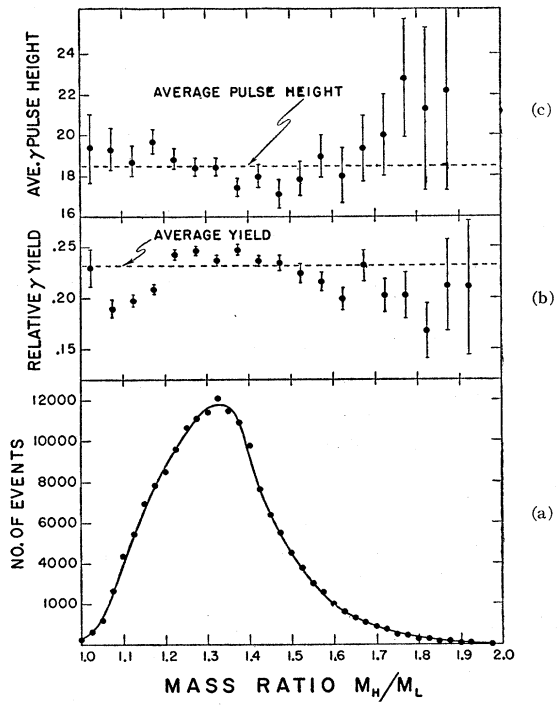

FIG. 8. (a) Mass-ratio distribution. (b) Yield of gamma-ray pulse heights greater than 200 kev in the 4-in. crystal. (c) Average height of all pulses in the range 200 to 1400 kev.

[14] R. S. Burington and D. C. May, *Handbook of Probability and Statistics* (Handbook Publishers, Inc., Sandusky, 1953), p. 181.
[15] C. O. Muehlhause, Phys. Rev. **79**, 277 (1950).
[16] Hicks, Ise, Pyle, Choppin, and Harvey, Phys. Rev. **105**, 1507 (1957).

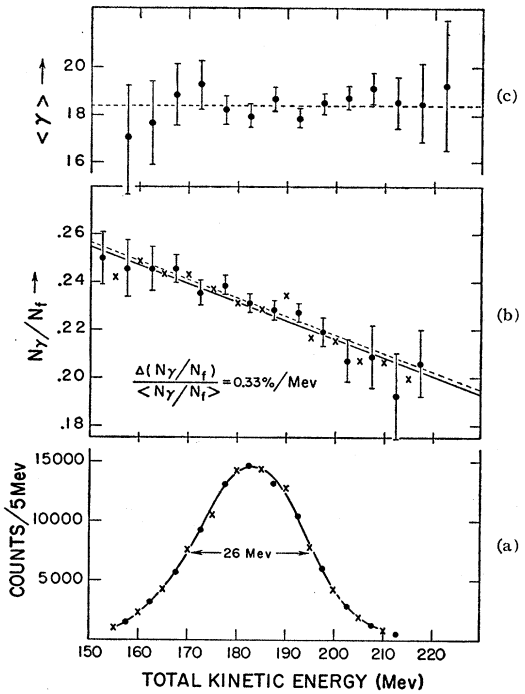

FIG. 9. (a) Distribution of total kinetic energies. [See note in caption of Fig. 4(a).] (b) Yield of gamma-ray pulse heights greater than 200 kev. The crosses represent one set of "extra" points and the dotted line is a least-squares fit to them. (c) Average height of all pulses in the range 200 to 1400 kev.

A small correction must be applied for the effect of neutrons on the NaI detector. The effective cross section for production of pulses greater than 200 kev by fission neutrons has been estimated to be <1 barn, using the inelastic neutron cross sections of Cranberg *et al.*[17] Using the value $d\langle\nu\rangle/dE_T=-0.08$ selected as a reasonable value from Hicks *et al.*,[16] and, taking into account that on the average there are four neutrons and nine gamma rays,[18] and that the solid angle for neutrons is less than half that for gamma rays at 90° to the fragment direction, we find that

$$\left|\frac{1}{\langle N_\gamma\rangle}\frac{dN_\gamma}{dE_T}\right|_{\text{neutron}}<0.0004\ \text{Mev}^{-1}.$$

The corrected variation in gamma-ray yield is thus

$$\frac{1}{\langle N_\gamma\rangle}\frac{dN_\gamma}{dE_T}=-0.0029\pm0.0005_{-0.0006}{}^{+0.0002}\ \text{Mev}^{-1},$$

where the first error is statistical and the second the uncertainty in the correction. There seems to be no significant trend in the average gamma pulse height as a function of E_T.

[17] Cranberg, Day, Rosen, Taschek, and Walt, in *Progress in Nuclear Energy* (McGraw-Hill Book Company, Inc., New York, 1956), Vol. I, p. 157.

[18] Smith, Fields, and Friedman, Phys. Rev. **104**, 699 (1956).

The experimental value for the rate of change of the gamma-ray yield with E_T may be compared with the value $dE_\gamma/dE_T=-0.0167$ deduced by Leachman and Kazek[19] through the relation

$$\frac{1}{\langle N_\gamma\rangle}\frac{dN_\gamma}{dE_T}=\frac{1}{\langle E_\gamma\rangle}\frac{dE_\gamma}{dE_T}=-\frac{0.0167}{4}=-0.0042\ \text{Mev}^{-1},$$

assuming that the average photon energy is constant [see Fig. 9(c)]. Leachman and Kazek deduced their value from an evaporation calculation made to fit the observed neutron multiplicities. The prediction of the model that the amount of energy going into gamma emission is very nearly constant is experimentally verified.

SINGLE-FRAGMENT VELOCITY AND ENERGY DISTRIBUTIONS

In many types of experiments it is feasible to measure only the single-fragment energy distributions. The single-fragment time-of-flight spectrum is obtained directly in this experiment and the energy distribution is easily derived. It is clear from Figs. 10 and 11 that the light and heavy fragment groups are more clearly separated in the time-of-flight representation. The difference is inherent in the shape and orientation of the probability of splitting $P(t_1,t_2)$. The way in which this effect arises may be seen by referring to Fig. 2. Slices taken along the lines of constant mass ratio separate the light and heavy groups best; slices along lines of constant time-of-flight are almost as good, while slices along the lines of constant kinetic energy are quite poor. (These lines are not shown on the diagram; they intersect the line $R=1$ at about 60° and 120°.) For instance, a fragment with 92 Mev has an appreciable probability of being either a light fragment associated

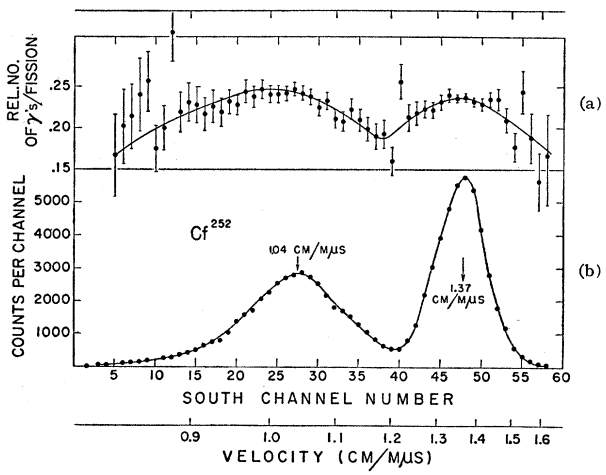

FIG. 10. (a) Single-fragment time-of-flight spectrum. (b) Gamma-ray yield as a function of single-fragment time of flight.

[19] R. B. Leachman and C. S. Kazek, Jr., Phys. Rev. **105**, 1511 (1957).

with low total kinetic energy or a heavy fragment associated with high total kinetic energy. The valley between light- and heavy-fragment peaks is therefore deeper in the time-of-flight plot than in the kinetic-energy plot. As a consequence, the gamma-ray yields show more structure as a function of time of flight than of energy, because the single time of flight is selecting a narrower region of E_T.

The most probable light- and heavy-fragment energies are found to be 104.7±1 and 79.8±1 Mev, respectively.

DISCUSSION

The observed width of the kinetic energy distribution at the most probable mass ratio is 17.5±1.0 Mev. This value is significantly larger than the 13.4±2.7 Mev found by Stein[4] for the thermal-neutron fission of U^{235}. Both values are consistent with those required in a description by the evaporation model of the emission of neutrons from excited fission fragments.[20,21] The larger spread in kinetic energy (and therefore, presumably, in excitation energy) is reflected in the fact that the variance of the prompt neutron number distribution is larger in Cf^{252} (1.54±0.04) than in U^{235} (1.22±0.04).[21] Calculations on neutron and gamma emission from fission fragments using the evaporation model are being carried out and will be submitted for publication shortly.

It appears that some shell effects are exhibited in the prompt-fission-fragment energy distributions. In particular, magic-number nuclei seem to give fewer gamma rays with perhaps slightly greater average energy. There also appears to be a slight influence on the mass yield. In contrast to the case of neutron emission, the variation in number and energy of the gamma rays with total kinetic energy is very small. The order of magnitude and sign of the change is correctly predicted by neutron evaporation calculations, which nevertheless give values of the total energy going into gamma rays which are too low by a factor of two.[18,19]

The time-of-flight technique as a method of defining prompt masses and energies of fission fragments has been pushed nearly to its limit. In order to reduce the uncertainty introduced by the prompt-neutron recoil, it is necessary to add further complications such as magnetic separators or simultaneous measurement of neutron velocities and angles of emission, with a consequent reduction in counting rate. Currently available spontaneous-fission sources do not permit such a reduction in counting rate, but thermal-neutron fission sources may make such experiments feasible. The present resolution was, however, sufficient to indicate for the first time some closed-shell effects in the prompt fragments.

[20] R. B. Leachman, Phys. Rev. **101**, 1005 (1956).
[21] J. Terrell, Phys. Rev. **108**, 783 (1957).

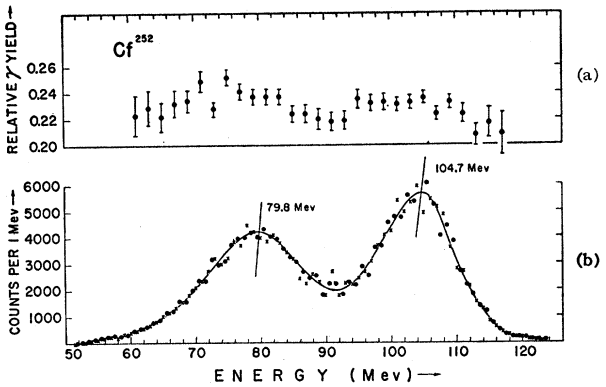

FIG. 11 (a) Single-fragment energy spectrum. [See note in caption of Fig. 4(a).] (b) Gamma-ray yield as a function of single-fragment energy.

ACKNOWLEDGMENTS

It is a pleasure to thank Mrs. W. F. Merritt for making many fine VYNS films; Dr. J. M. Kennedy and Mrs. E. A. Okazaki for help with the Datatron. We are indeed most grateful to Dr. S. G. Thompson of the University of California Radiation Laboratory for providing us with the Cf^{252} source used in this experiment.

APPENDIX A. LONGITUDINAL COMPONENT NEUTRON RECOIL[22]

We define M_f, the fragment mass; M_n, the neutron mass; η, the neutron energy in the center-of-mass system; ϑ, π minus the angle between the neutron and the fragment in the center-of-mass system; and V_f, the fragment velocity. We assume that the angular distribution of the neutrons (c.m. system) is given by $1+A_2P_2(\cos\vartheta)$ and that the energy spectrum (c.m. system) is[23]

$$\varphi(\eta)=(1/T^2)\eta e^{-\eta/T},$$

where T is a constant to be determined and has the dimensions of energy. Then, since the neutron momentum is small compared to that of the fragment, the longitudinal component of fragment momentum change is

$$y=(2M_n\eta)^{\frac{1}{2}}\cos\vartheta.$$

It can then be shown that the distribution in these momentum changes, $R(y)$, is given by

$$(2M_nT)^{\frac{1}{2}}R(y)=(1-A_2/2)f(z)+A_2g(z), \qquad (1)$$

[22] The calculations in Appendices A and B are given in more detail, along with others on laboratory neutron spectra, in Chalk River Laboratory Report CRP-740 (unpublished).
[23] J. M. Blatt and V. F. Weisskopf, *Theoretical Nuclear Physics* (John Wiley and Sons, Inc., New York, 1952), p. 365 ff.

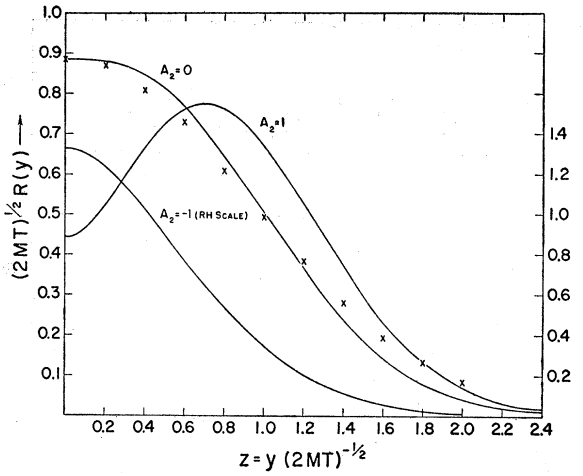

FIG. 12. The distribution $R(y)$ in the longitudinal component y of fragment recoil momenta, for $A_2=+1$, 0, -1.

where

$$z=(2M_nT)^{-\frac{1}{2}}y,$$

$$f(z)=z\exp(-z^2)+\pi^{\frac{1}{2}}[\tfrac{1}{2}-\operatorname{erf}(\sqrt{2}z)],$$

$$g(z)=3\pi^{\frac{1}{2}}z^2[\tfrac{1}{2}-\operatorname{erf}(\sqrt{2}z)],$$

$$\operatorname{erf}t=(2\pi)^{-\frac{1}{2}}\int_0^t\exp(-x^2/2)dx.$$

$R(y)$ is illustrated in Fig. 12 for three values of A_2. We notice that on the average the fragment velocity is not changed by neutron emission. In this paper we will confine ourselves to the case $A_2=0$, i.e., isotropic neutron emission. In this case the full width at half maximum $z_{\frac{1}{2}}$ is 2.17 and the distribution is nearly Gaussian. It is now quite simple to relate changes in velocity to z:

$$\frac{\Delta V_f}{V_f}=\frac{y}{M_fV_f}=\frac{(1+R)(M_nT)^{\frac{1}{2}}}{(RM_TE_T)^{\frac{1}{2}}}z, \tag{2}$$

where M_T is the mass of the fissioning nucleus, R is the mass ratio, and E_T the total kinetic energy. For Cf^{252} we get, for the relative full width at half-maximum,

$$(\Delta V_f/V_f)_{\frac{1}{2}}=0.0203(\nu T)^{\frac{1}{2}} \tag{3}$$

after ν neutrons have been emitted. The numerical constant applies to $R=1.33$, but a range of 9.5% about this value includes 85% of all the fissions.

The parameter T is determined by fitting the laboratory neutron spectrum.[22] We have used the data of Smith, Fields, and Roberts.[24] It is not possible to fit the results with a single temperature, so we have made a least-squares fit to α, T_1, and T_2 using an energy spectrum in the c.m. system:

$$\varphi(\eta)=\frac{\alpha}{T_1^2}\eta e^{-\eta/T_1}+\frac{1-\alpha}{T_2^2}\eta e^{-\eta/T_2}.$$

This should be considered as an empirical expression for the c.m. spectrum. The procedure of fitting $\varphi(\eta)$ to the laboratory spectrum ensures that the final result is not sensitive to the analytic form assumed. The values are $\alpha=0.5504$, $T_1=1.059$ Mev, $T_2=0.3861$ Mev. From this, $T_{\text{eff}}{}^{\frac{1}{2}}$ is estimated to be 0.866 $(\text{Mev})^{\frac{1}{2}}$. From a plot of $\sum P_\nu R_\nu(y)$ we find, using the probabilities $P(\nu)$ given by Hicks *et al.*,[16] that $\nu_{\text{eff}}{}^{\frac{1}{2}}=1.80$. The width calculated this way is a little narrower than would be obtained by putting $\langle\nu\rangle$ in Eq. (3). The final result is

$$(\Delta V_f/V_f)_{\frac{1}{2}}=0.0314.$$

In an identical manner, the velocity spread for the slow-neutron fission of U^{235} is calculated to be

$$(\Delta V_f/V_f)_{\frac{1}{2}}=0.026.$$

The mass resolution is then found through the relation

$$\Delta M=\frac{M_TR}{(1+R)^2}(1+R^2)^{\frac{1}{2}}\left(\frac{\Delta v_H}{v_H}\right),$$

and the total kinetic-energy spread by

$$\frac{\Delta E}{E}=\left[\left(\frac{\Delta v_1}{v_1}\right)^2+\left(\frac{\Delta v_2}{v_2}\right)^2\right]^{\frac{1}{2}}.$$

Before leaving this section we observe that if A_2 were as large as $+1$, i.e., predominantly forward and backward emission of neutrons, the spread in total kinetic energy would be 10% for Cf^{252}. If we use the observed width of 20 Mev at $R=1.33$, only 7.5 Mev spread in E_T would be left to give a spread in the fragment excitation energies. This is totally inadequate to give the known variation in the number of neutrons.[5,16]

APPENDIX B. DEFLECTION OF THE FRAGMENTS BY NEUTRON RECOIL

After a flight path L, the deflection of the fragment in the plane of the detector from the point collinear with its partner fragment, which has not emitted a neutron, is

$$\rho=\frac{1+R}{R^{\frac{1}{2}}}\left(\frac{M_n}{M_TE_T}\right)^{\frac{1}{2}}L\eta^{\frac{1}{2}}\sin\vartheta, \tag{4}$$

where ρ is in the same units as L and $\rho/L\ll1$. We define a quantity x by

$$\rho=x\eta^{\frac{1}{2}}\sin\vartheta.$$

For Cf^{252}, $x=0.6718$ for the flight path of 71.8 inches used in this experiment and is a very slowly varying function over the distribution of R and E_T. We there-

[24] Smith, Fields, and Roberts, Phys. Rev. **108**, 411 (1957).

fore assume that all the variation in ρ is due to η and ϑ. (This assumption has been checked by a Monte Carlo calculation and found to introduce negligible error.[22])

With the same definitions as in Appendix A, it can be shown that the distribution in deflections is given by

$$D(\rho)=(1+A_2)v(\rho)-A_2w(\rho), \tag{5}$$

$$v(\rho)=\frac{\rho}{x^2T^2}\int_{\rho^2/x^2}^{\infty}\frac{\eta^{\frac{1}{2}}e^{-\eta/T}d\eta}{(\eta-\rho^2/x^2)^{\frac{1}{2}}},$$

$$w(\rho)=-\frac{3}{2}\frac{\rho^3}{x^4T^2}\int_{\rho^2/x^2}^{\infty}\frac{\eta^{-\frac{1}{2}}e^{-\eta/T}d\eta}{(\eta-\rho^2/x^2)^{\frac{1}{2}}}.$$

$D(\rho)$ is shown in Fig. 13 for $T=1$ Mev. Although $D(\rho)$ is a long way from being Gaussian, nevertheless, from an examination of the first four moments about the origin it has been shown that after ν neutrons have been emitted, the distribution is given very closely by

$$D_\nu(\rho)=\nu^{-\frac{1}{2}}D(\nu^{\frac{1}{2}}\rho), \tag{6}$$

where the second moment of the right side of Eq. (6) is identical with that of the true distribution and the first moment (the average) is 1.4% low for $\nu=2$.

The efficiency of two finite-sized detectors separated by a distance $2L$ was next calculated for a point source by using a Monte Carlo method and the distributions $D_\nu(\rho_\nu)$ of Eq. (6). One of the detectors was assumed to have a radius r, and the distribution in ρ_ν was calculated in the plane of the other detector. The calculation has been made for Cf^{252} and U^{236}. The results for Cf^{252} are shown in Fig. 14.

Since the efficiency varies with ν, the value of any quantity which is correlated with ν must be corrected for the changing efficiency. Hicks *et al.*[16] have shown that there is almost no correlation between $\langle\nu\rangle$ and mass ratio, but that there is a strong correlation $\langle\nu\rangle$

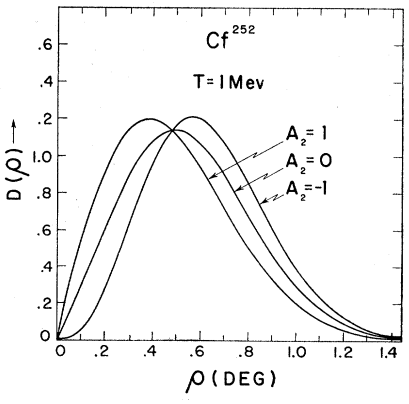

FIG. 13. The distribution in fragment deflection $D(\rho)$, where ρ is the angular deflection, for asymmetry coefficients $A_2=+1, 0, -1$, and $T=1$ Mev.

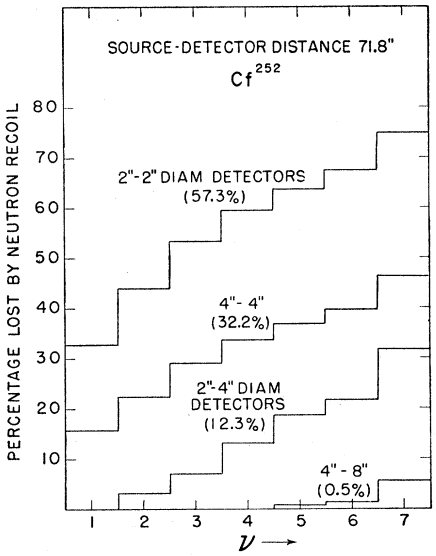

FIG. 14. The efficiency as a function of ν for four detector combinations. In all cases the detectors are each 71.8 in. from the source. The number in parentheses is the weighted average fraction lost.

with E_T such that

$$d\langle\nu\rangle/dE_T\approx-0.08\ \text{Mev}^{-1}.$$

Recently, Stein and Whetstone[5] have found

$$\partial\langle\nu\rangle/\partial E_T=-0.143\ \text{Mev}^{-1}\quad\text{and}\quad\partial\langle\nu\rangle/\partial R=-6.3.$$

Under the assumptions that the efficiency ϵ varies linearly with ν and that ν varies linearly with some observable quantity, x, it can be shown that the change change of the observed average from the true average is given by

$$\langle x\rangle_{\text{obs}}-\langle x\rangle=\frac{\sigma_x^2}{\langle\epsilon\rangle}\frac{\partial E}{\partial\nu}\frac{\partial\nu}{\partial x},$$

where $\sigma_x^2=\langle x^2\rangle-\langle x\rangle^2$. $\langle\epsilon\rangle$ and $\partial\epsilon/\partial\nu$ are found from the calculation already described; σ_x is assumed to be given closely enough by the observed width of the total kinetic-energy distribution.

With $\partial\langle\nu\rangle/\partial E_T=-0.1\pm0.05$ and $\sigma=11$ Mev, the correction to the average total kinetic energy is

$$\langle E_T\rangle_{\text{obs}}-\langle E\rangle=0.8\pm0.4\ \text{Mev}$$

for the 4-in. detectors used in this experiment. If only a narrow band of energies is considered, $d\langle\nu\rangle/dR$ is large and the shift in the average value of the mass ratio is

$$\langle R\rangle_{\text{obs}}-\langle R\rangle=0.007.$$

This is small enough to be neglected. If a wide range of energies is considered, $d\langle\nu\rangle/dR$ is small[5] and the shift in R is correspondingly smaller. The over-all mass distribution is therefore not affected by the variation in efficiency with ν.